Postprint of a Study on Measurement of Thermal Expansion Coefficient Using Electrostatic Levitation Containerless Method

Authors: Sun Yining, Wang Feilong, Sun Zhibin, Yu Qiang, Zhai Guangjie

Date: 2017-03-10T00:00:00+00:00

Abstract

Traditional contact measurement methods are incapable of measuring the thermal expansion coefficient of metallic materials within the high-temperature range. By combining electrostatic levitation containerless technology with image measurement methods, the levitated sample is heated using a semiconductor laser. During the heating process, images of the levitated sample are captured using a CCD camera, the sample edges in the images are extracted via a directional gradient algorithm, and the sample volume is fitted using spherical harmonic functions to calculate the thermal expansion coefficient of the material at various temperatures. Experiments were performed using pure zirconium metallic samples; within the temperature range of 750-1800°C, the temperature-dependent expression for the thermal expansion coefficient of solid-state zirconium samples was measured and obtained, thereby validating the effectiveness and precision of this measurement method.

Full Text

Preamble

Containerless Measurement of Thermal Expansion by Electrostatic Levitation

Wang Feilong[12], Sun Yining[12], Sun Zhibin[1], Yu Qiang[1], Zhai Guangjie[1]

[1]Key Laboratory of Electronics and Information Technology for Space Systems, National Space Science Center, Chinese Academy of Sciences, Beijing 100190, China
[2]University of Chinese Academy of Sciences, Beijing 100049, China

Abstract: Traditional contact methods cannot measure the thermal expansion coefficients of metallic materials at high temperatures. This study combines containerless electrostatic levitation with image measurement techniques. During heating, a CCD camera records images of the levitated sample, which is heated by a semiconductor laser. A directional gradient algorithm extracts the sample edge from the images, and spherical harmonic functions are fitted to calculate the sample volume, enabling determination of the material' s thermal expansion coefficient at various temperatures. Experiments using pure zirconium demonstrate the method' s validity and accuracy across 750–1800°C.

Keywords: thermal expansion coefficient; containerless method; image processing; thermophysical properties measurement

0 Introduction

The thermal expansion coefficient is a fundamental thermophysical parameter of materials and a critical factor in engineering design, precision instrument manufacturing, welding, and materials processing that cannot be ignored [**?**, **?**]. Conventional measurement techniques, including push-rod methods, interferometry, and dilatometry [**?**], rely on contact heating through thermal conduction. These approaches suffer from limited maximum temperatures and poor temperature uniformity at elevated temperatures, which compromises measurement precision and restricts the effective temperature range (generally below 1500 K).

Since the 1960s, containerless non-contact measurement techniques, exemplified by electromagnetic levitation, have been applied to thermophysical property characterization [**?**]. Containerless methods utilize gas flow [**?**], acoustic fields [**?**], electromagnetic fields [**?**], or electrostatic fields [**?**, **?**] to suspend samples, eliminating contact with container walls. High-power lasers enable heating to much higher temperatures, even beyond the melting point, while the unobstructed, levitated state facilitates high-precision volumetric measurements through imaging. For high-temperature metallic materials, high-vacuum environments are essential: vacuum conditions allow radiative cooling to achieve higher temperatures and prevent oxidation that would affect measurement accuracy. Aerodynamic and acoustic levitation are unsuitable for vacuum environments, while electromagnetic levitation couples suspension and heating, preventing independent temperature control and limiting low-temperature measurements. Additionally, eddy currents in electromagnetic fields destabilize molten sample shapes, reducing measurement precision.

This work employs an electrostatic levitation facility for thermal expansion coefficient measurements [**?**]. Electrostatic levitation overcomes electromagnetic levitation limitations by enabling independent heating control and maintaining stable sample configurations from heating through melting. The system uses a CCD camera with background illumination to capture clear side-view images, from which volume changes are calculated through image processing algorithms.

The measurement system is validated and tested through experiments with pure zirconium samples.

1 Experimental Apparatus

Thermal expansion coefficient measurements are performed on an electrostatic levitation materials science platform comprising a vacuum chamber, levitation position control system, heating laser, dual-wavelength pyrometer, and CCD camera. The system configuration is shown in

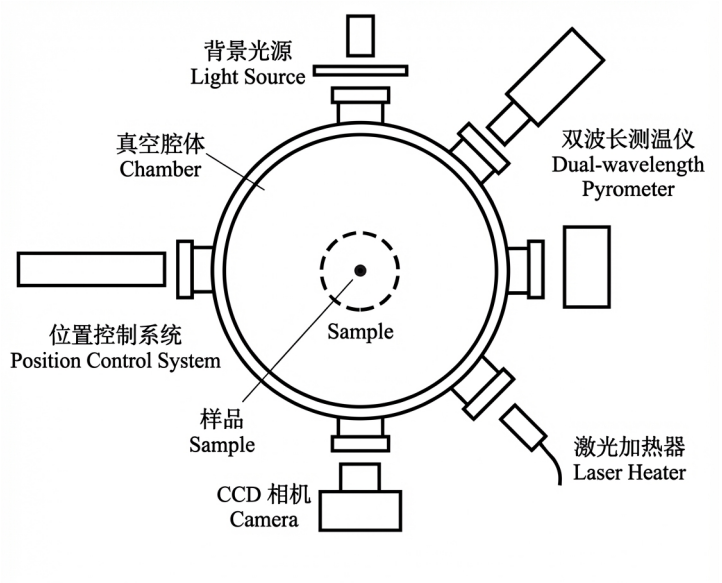

Fig. 1 Schematic diagram of the electrostatic levitation device

Figure 1: Figure 1

. The vacuum chamber maintains a high-vacuum environment below 5$×10^{-5}$ Pa using a mechanical pump and turbomolecular pump. Test materials are spherical samples 2–3 mm in diameter. Inside the chamber, a pair of high-voltage parallel plates spaced 10 mm apart generates an electric field that levitates charged samples via Coulomb force, counteracting gravity. Sample position is stabilized through a feedback control system [**?**].

Once stable levitation is achieved, the sample is heated by a laser heater while temperature is monitored by a dual-wavelength pyrometer. An 808 nm high-power semiconductor laser with 90 W output is fiber-coupled and focused onto the sample surface, achieving maximum temperatures of 2500°C for metallic materials. Temperature measurement employs a dual-wavelength pyrometer (SensorTherm MQ22) sampling at 50 Hz, which calculates temperature from the ratio of radiance at two adjacent wavelengths, making it independent of

emissivity and measurement solid angle for high accuracy. Thermal expansion coefficients are determined during heating through the image acquisition system.

At elevated temperatures, the sample emits intense visible light that blurs image edges. To obtain clear contours, a halogen lamp with frosted glass provides background illumination that mitigates self-luminosity effects. Because the sample remains containerless, even molten samples maintain near-spherical shapes due to surface tension. Leveraging this spherical axisymmetry, side-view images suffice for precise volume determination through image processing algorithms [**?**].

2 Image Processing Algorithm

Precise volume measurement from sample images requires sophisticated image processing. First, the sample edge must be extracted from the background. Edge detection relies on gradient changes in pixel intensity [**?**], but gradients are directional. Conventional methods calculate gradients along horizontal and vertical axes, which proves insufficient for circular edges. For spherical samples, the most pronounced gradient occurs perpendicular to the edge tangent. Therefore, this system employs a directional gradient algorithm tailored to circular features.

The algorithm generates 360 directional vectors radiating from an approximate center, which can be initially approximated by the center of the sample' s bounding rectangle. Along each vector direction, a sequence of pixels with directional characteristics is sampled. The pixel sequences along the 360 directional vectors are expressed as:

MATH_0

where i indexes the 360 directional vectors, j indexes pixels along each vector, x and y are horizontal and vertical pixel coordinates, and r is the radius for pixel sequence generation. Since image pixels are discrete, radius r increments by one pixel until reaching the image boundary.

Each two-dimensional pixel sequence is processed as a one-dimensional grayscale array. Differentiating the grayscale values yields gradient changes along that direction, with the edge located at the pixel position of maximum gradient. This process yields 360 edge pixel coordinates MATH_1 . To improve edge extraction precision, the average of the x and y coordinates serves as a new approximate center MATH_2 . The process repeats using this refined center to regenerate the 360 vectors and re-detect edge pixels. The final edge extraction result using the directional gradient algorithm is shown in

.

The extracted edge information consists of discrete pixel coordinates. Even with high-resolution CCD acquisition, the discrete nature of pixels introduces jagged edges that affect precise volume calculation. The system addresses this

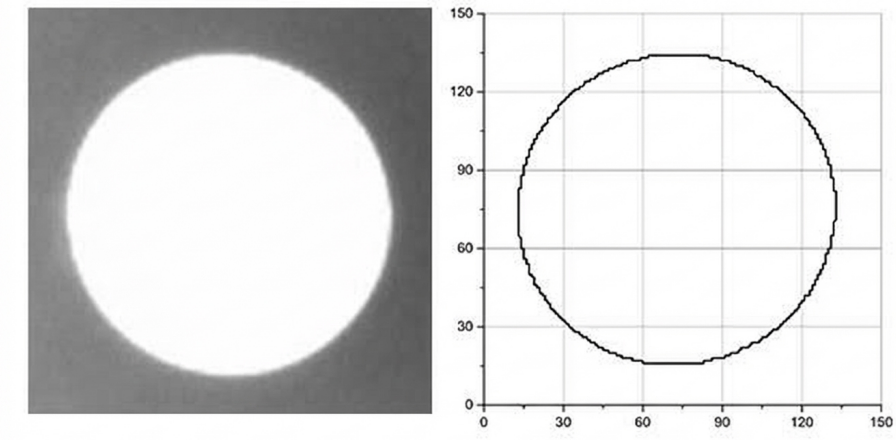

Fig. 3 Edge extraction of sample image using directional gradient algorithm

Figure 2: Figure 3

through spherical harmonic function fitting, which determines accurate spherical harmonic representations from limited discrete coordinates. The spherical harmonic representation is:

MATH_3

where MATH_4 is the Legendre polynomial of order n. Higher orders increase fitting accuracy but also computational load; the system employs 6th-order fitting, with MATH_5 representing coefficients to be determined.

For spherical harmonic fitting, edge pixels must be converted from Cartesian to polar coordinates:

MATH_6

where MATH_7 and MATH_8 are horizontal and vertical pixel metric coefficients (mm/pixel), representing the physical distance between pixels. These parameters depend on the CCD chip, sample distance, and lens focal length, and are calibrated using a standard-sized sample. MATH_9 and MATH_{10} are the precise pixel coordinate centers determined through fitting. Equation (3) transforms sample edge points to polar coordinates MATH_{11} .

Using the angular coordinate MATH_{12} , coefficients in Equation (2) are fitted to the polar coordinate points. The fitting parameters include Legendre polynomial coefficients MATH_{13} through MATH_{14} and coordinate centers MATH_{15} and MATH_{16} , obtained by minimizing the objective function:

MATH_{17}

where, for each angular direction MATH_{18} , the squared difference between the sample edge radius and the corresponding spherical harmonic radius is summed across 360 data sets. The minimum of this objective function yields the optimal fitting coefficients. Initially, MATH_{19} and MATH_{20} are set to the average of all pixel horizontal and vertical coordinates. Based on Equation (MATH_{21}), the fitting is linear with respect to coefficients MATH_{22} through MATH_{23} , enabling solution via least squares to obtain optimal coefficients for the initial center. The values of MATH_{24} and MATH_{25} are then varied incrementally; each change requires recalculating polar coordinate points via Equation (3) and reapplying least squares to determine a new set of Legendre polynomial coefficients that minimize the objective function.

After obtaining optimal spherical harmonic coefficients, sample volume is calculated by integrating the image contour radius:

MATH_{26}

The algorithm processes each image through batch processing. Using Equation (5), sample volume is computed and combined with temperature data to generate the volume-temperature curve shown in

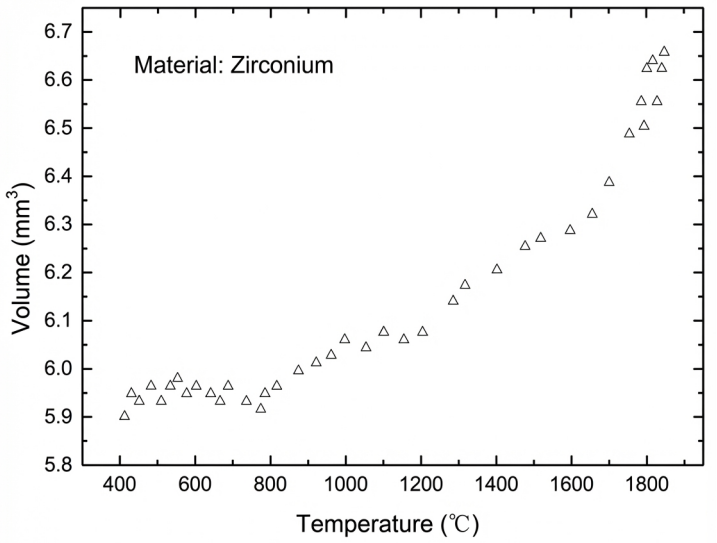

Fig. 5 Curve of Sample Volume Change with Temperature

Figure 3: Figure 5

.

Measurement precision is poorer in low-temperature stages and near the melting

point, so these regions are excluded from calculations. The thermal expansion coefficient is calculated from the volume-temperature data using Equation (6). The resulting relationship between thermal expansion coefficient and temperature is shown in

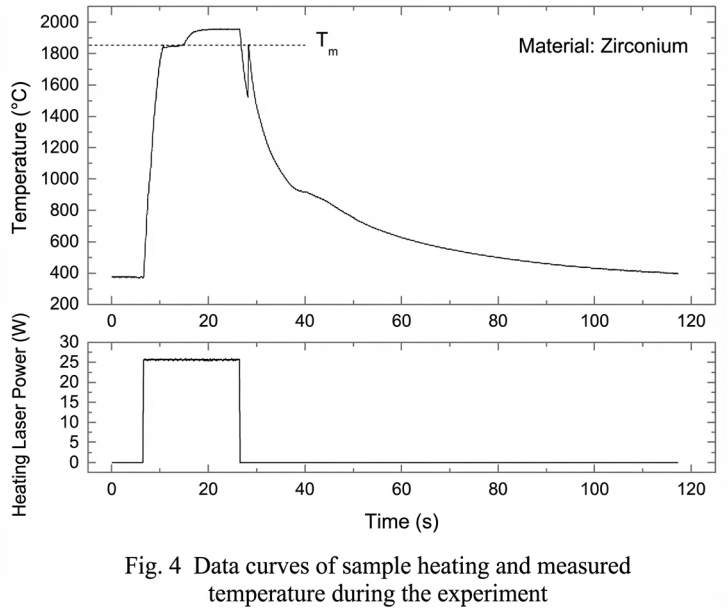

Fig. 4 Data curves of sample heating and measured temperature during the experiment

Figure 4: Figure 6

.

After obtaining sample volume and acquiring temperature variation data from the dual-wavelength pyrometer, the material's expansion coefficient is calculated using:

MATH_{27}

3 Experimental Process and Results

Before experiments begin, a standard-sized stainless steel sphere is levitated to calibrate the image acquisition system resolution. With the calibration sample stably levitated, the CCD camera' s aperture, focal length, and image contrast are adjusted for optimal clarity. These optical parameters remain fixed throughout subsequent experiments. By measuring the pixel count of the standard sample, the horizontal and vertical pixel metric coefficients MATH_{28} and MATH_{29} in Equation (3) are determined.

Following calibration, a pure zirconium sample (99.99% purity) prepared by vacuum arc melting is loaded. With the sample stably levitated, the semiconductor

laser heats it until complete melting, after which the heating laser is turned off. The sample then cools radiatively, solidifies, and exhibits recalescence. The measured melting point temperature (MATH_{30} = 1852°C) agrees with zirconium' s known melting point. The temperature data recorded during laser heating and pyrometry are shown in

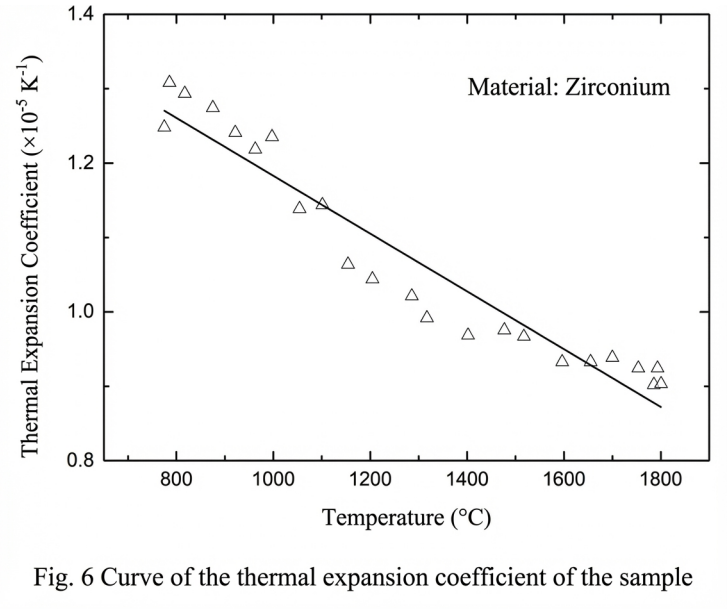

Fig. 6 Curve of the thermal expansion coefficient of the sample

Figure 5: Figure 4

.

The pyrometer acquisition period is 20 ms; each temperature reading triggers synchronized image acquisition. Image data and corresponding temperature information are stored on computer hard disk for post-experiment processing. Since the levitation system maintains position stability within $±$0.2 mm, the image processing region can be selected based on the first frame.

Because thermal expansion coefficient calculation is independent of sample mass, its precision depends solely on volumetric image measurement accuracy and dual-wavelength pyrometer precision. Least squares linear fitting of the data in

yields the temperature-dependent expression for solid zirconium' s thermal expansion coefficient:

MATH_{31}

where the sample' s thermal expansion coefficient MATH_{32} has units of MATH_{33} and sample temperature MATH_{34} has units of MATH_{35} .

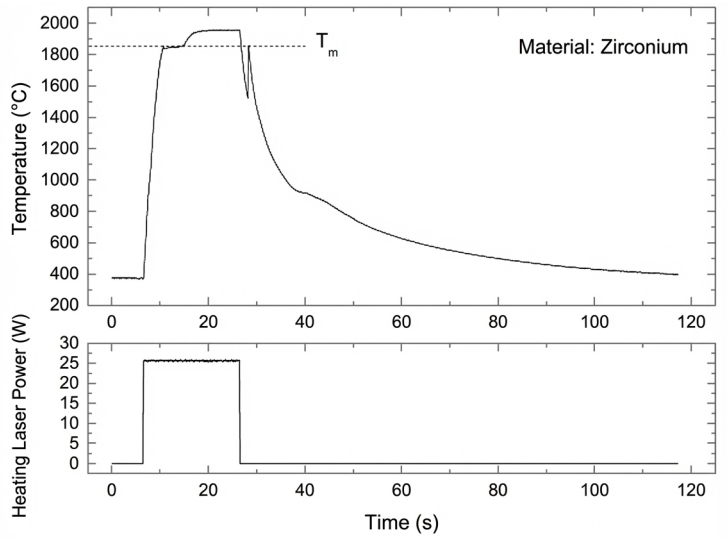

Fig. 4 Data curves of sample heating and measured temperature during the experiment

Figure 6: Figure 6

4 Conclusion

This paper demonstrates measurement of metallic materials' thermal expansion coefficients using electrostatic levitation, extending the effective temperature range beyond 2000 K compared to traditional methods. The approach achieves higher precision than other containerless techniques like electromagnetic levitation. Background illumination enhances edge contrast in acquired images, while gradient-based edge extraction and spherical harmonic fitting algorithms further improve volumetric measurement accuracy. Validation through zirconium experiments confirms the method' s effectiveness, providing researchers across various fields with precise thermal expansion coefficient data and measurement methodologies for high-melting-point alloys.

References

[1] Chen Guisheng, Liao Yan, Zeng Yaguang, et al. Research status and development requirements for material thermophysical property testing[J]. China Measurement & Test, 2010, 36(5): 5-8.

[2] Zhu Yuying, Li Qiang, He Yunhua, et al. Study on thermophysical properties of undercooled melts using containerless solidification technology[J]. Materials Review, 2009, 23: 78-81.

[3] Yang Xinyuan, Sun Jianping, Zhang Jintao. Introduction to modern development and method comparison for material linear thermal expansion coefficient

measurement[J]. Measurement Technique, 2008(7): 33-36.

[4] Wang Qing, Dai Jianfeng, Li Weixue, et al. A new method for measuring metal thermal expansion coefficients[J]. Physics, 2003(10): 32-34.

[5] Hu Liang, Lu Xiaoyu, Hou Zhimin. Research progress in electrostatic levitation technology[J]. Physics, 2007, 36(12): 944-950.

[6] Weber J K R, Hampton D S, Merkley D R, et al. Aero-acoustic levitation: A method for containerless liquid-phase processing at high temperatures[J]. Review of Scientific Instruments, 1994, 65(2): 456.

[7] Tian Y, Holt R G, Apfel R E. A new method for measuring liquid surface tension with acoustic levitation[J]. Review of Scientific Instruments, 1995, 66(5): 3349-3354.

[8] Okress E C, Wroughton D M, Comenetz G, et al. Electromagnetic levitation of solid and molten metals[J]. Journal of Applied Physics, 1952, 23(5): 545-552.

[9] Rhim W K, Chung S K, Barber D, et al. An electrostatic levitator for high-temperature containerless materials processing in 1-g[J]. Review of Scientific Instruments, 1993, 64(10): 2961-2970.

[10] Wang F L, Dai B, Liu X F, et al. Containerless heating process of a deeply undercooled metal droplet by electrostatic levitation[J]. Chinese Physics Letters, 2015(11): 39-42.

[11] Dai Bin, Sun Zhibin, Wang Feilong, et al. Design of electrostatic levitation position measurement and control system based on PSD[J]. Sensors and Microsystems, 2015, 34(3): 97-99.

[12] Li Xiaohua. MEMS micro-droplet volume measurement method based on image processing[J]. China Measurement & Test, 2014(04): 37-41.

[13] Tang Yanli, Su Yanchen. Application of digital image processing in distance measurement[J]. China Measurement & Test, 2009, 35(1): 63-67.

Figures

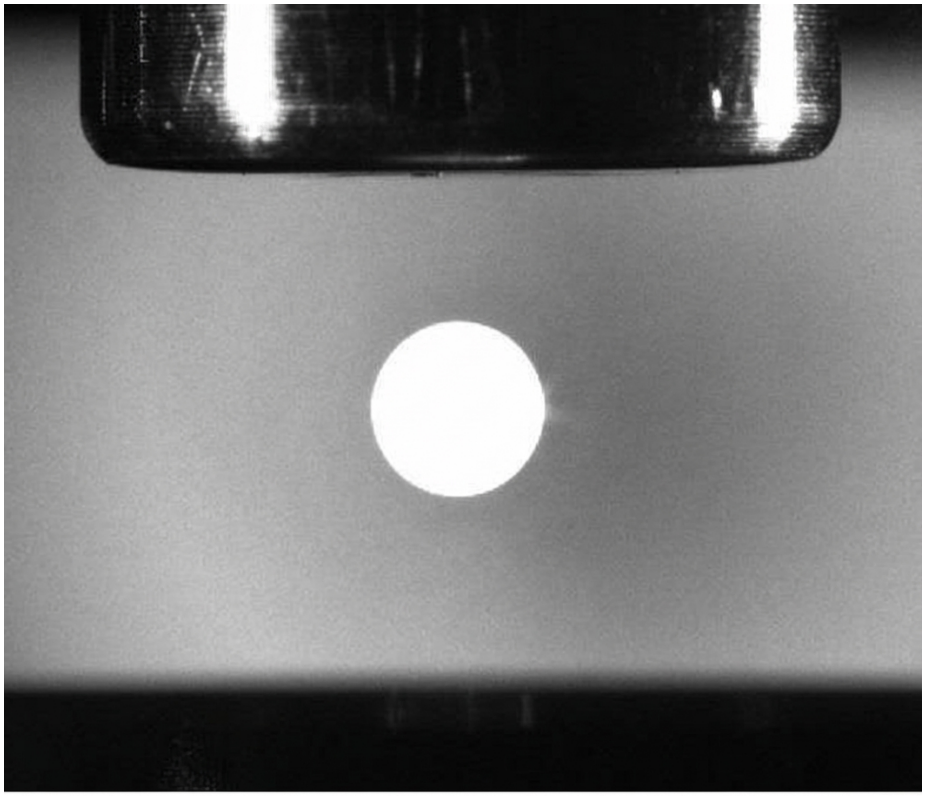

Figure 2 Image of the heated sample captured by CCD camera

Figure 7: Figure 2